Paper
Int'l J. of Aeronautical & Space Sci. 17(3), 378–390 (2016)
DOI: http://dx.doi.org/10.5139/IJASS.2016.17.3.378

IJASS
International Journal of Aeronautical and Space Sciences

Perch Landing Assisted by Thruster (PLAT): Concept and Trajectory Optimization

Min-Jea Tahk*, Seungyeop Han, Byung-Yoon Lee*** and Jaemyung Ahn******

Department of Aerospace Engineering, Korea Advanced Institute of Science and Technology, Daejeon 34141, Republic of Korea

Abstract

A concept of the perch landing assisted by thruster (PLAT) for a fixed wind aircraft is proposed in this paper. The proposed concept is applicable to relatively large unmanned aerial vehicles (UAV), hence can overcome the limitation of existing perch landing technologies. A planar rigid body motion of an aircraft with aerodynamic and thruster forces and moments is modeled. An optimal control problem to minimize the fuel consumption by determining the histories of thruster and elevator deflection angle with specified terminal landing condition is formulated and solved. A parametric study for various initial conditions and thruster parameters is conducted to demonstrate the practicability of the proposed concept.

Key words: Vertical Landing, Thrusters Assisted, Deep Stall, Optimal Control

1. Introduction

Recently, unmanned aerial vehicle (UAV) systems are widely used in regions where securing a runway is almost impossible such as mountain or marine area. However, fixed wing aircrafts inherently require a long distance runway due to their approach velocity, which must be above the stall speed. A number of different systems for short take-off and landing have been developed to overcome this limit. For take-off of an aircraft, the catapult and rail launcher with small rocket have been successfully demonstrated their usability [15].

Various landing technologies such as the parachutes method, the net-recovery method, the deep stall method and the perching method have been developed and actively explored so far. The parachute method has advantage in easiness of implementation, but it adds volume for parachute storage, and is relatively hard landing and is difficult to land precisely. In case of the net-recovery method, it can achieve "Zero-length" recovery, but it requires open area to secure the flight path and is also relatively hard landing. The deep stall method and perching method have strength in easiness of implementation and low cost of system, but both are relatively hard landing and only applicable to small size airplane [15].

As the aero-braking landing method, such as deep stall and perching, is quite simple to implement and very effective in reducing the velocity of a vehicle. This research first notices the concept and procedure of it. Deep stall landing in small size UAV in this work [10], longitudinal trim condition after deep stall of a small UAV was estimated as a function of horizontal tail plane angle and flight velocity. The UAV can have high flight path angle with low speed by maintaining this trim condition. A similar research on the deep stall landing using Micro Aerial Vehicles (MAV) suggests a criterion on landing or recovery decision [11]. However, these previous researches are only applicable to small size vehicles and cannot make zero velocity at a desired position. When the deep stall method is used for large size vehicles such as RQ7-Shadow or MQ1-Predator, large impact during touchdown procedure can occur, which jeopardize the whole system. In addition, the use of high angle of attack aerodynamic force/moment for landing attitude control increases the uncertainty in the vehicle's dynamic behavior.

A perch landing can be considered as an attractive alternative to the deep stall method. Crowther described a fixed wing aircraft perch landing as a three-phase procedure composed of the approach phase, the extended flare phase,

* Professor of Aerospace Engineering
** MS Student, Corresponding author: novelhan@kaist.ac.kr
*** Ph. D Student
**** Associate Professor of Aerospace Engineering

Received: February 4, 2016 Revised: May 12, 2016 Accepted: August 22, 2016

http://ijass.org pISSN: 2093-274x eISSN: 2093-2480

and the post stall capture phase [6]. In this study, a genetic algorithm (GA) is used to calculate the vehicle's trajectory and elevator input profile with specified final conditions for landing. To compute optimal perching trajectories, Wickenheiser and Garcia proposed a formulation composed of two phases – the dive phase and the climb phase [7]. In their work, the perching maneuver that minimizes the starting distance (during the dive phase) and the altitude gain (during the climb phase) is obtained. Venkateswara proposed a relatively simple single-phase optimization procedure that minimizes the length of perching maneuver [8]. It was demonstrated that the single-phase procedure outperforms the two-phase method in terms of the computation time and the quality of the obtained solution. Meanwhile, Cory successfully conducted the numerical simulation of perching and its flight test of by using a light glider with motion capture system [9]. However, like the case for the deep stall method, previous studies on the perch landing are not applicable to large size UAV. Furthermore, it requires an open area to approach during the dive phase and leveled platform to land during the climb phase, which are usually tough barriers to harsh regions like mountains.

Recently, a number of researchers are focusing on overcoming the limitation in landing of fixed wing aircraft. Among them, Tahk [1] developed a new landing concept applicable to medium size UAVs. His new concept, referred to as *perch landing assisted by thruster* (PLAT), uses both of the aerodynamic force and the thrust generated by a small solid rocket to effectively reduce the velocity and precisely land the vehicle at the desired position. The PLAT procedure consists of three phases – the approach phase, the deep stall phase and the thrusting phase in order. While the proposed procedure is similar to the soft lunar landing in that the thruster is used, leveraging of atmospheric force/moment for deceleration and attitude control is a key differentiator [12,13]. Compared to existing aero-braking landing researches, The PLAT overcomes several problems; weight limitation, stability issue at high angle of attack, landing precision and landing area.

As a following research of [1], an optimal control problem that minimizes the usage of overall thrust while satisfying soft landing conditions, with a point-mass assumption and control variables of thrust vector and pitch angle, is formulated in references [3-4]. Both Gauss Pseudo Spectral method and Euler Lagrange method are used to find the optimal solution of the formulated problem. Another follow-on study presented in reference [5] introduced a control algorithm for PLAT and consequent controller design based on results of improved aircraft and aerodynamic models [3-4]. Also the two degrees-of-freedom problem in reference [1] is extended to a three degrees-of-freedom problem, also both trajectory optimization and parametric study are conducted with additional considerations on the elevator effects in reference [2].

The overall structure of the paper takes form of four sections, including this introduction part and the rest of paper are organized as follows. Detail description of new concept, modeling of reference aircraft and modeling of high angle of attack aerodynamic are introduced at Section 2. In Section 3, longitudinal equation of motions, formulation of optimal control problem, used optimization methods and optimization result and analysis of the results are presented. Finally, Section 4 covers concluding remarks as well as introduces a future work.

2. Perch Landing Assisted by Thruster

2.1 PLAT Description

The three phases of PLAT (approach phase, deep stall phase, and thrusting phase) and the thruster configuration required for this approach are presented in Fig. 1-(a) and Fig. 1-(b), respectively [1]. We propose a configuration composed

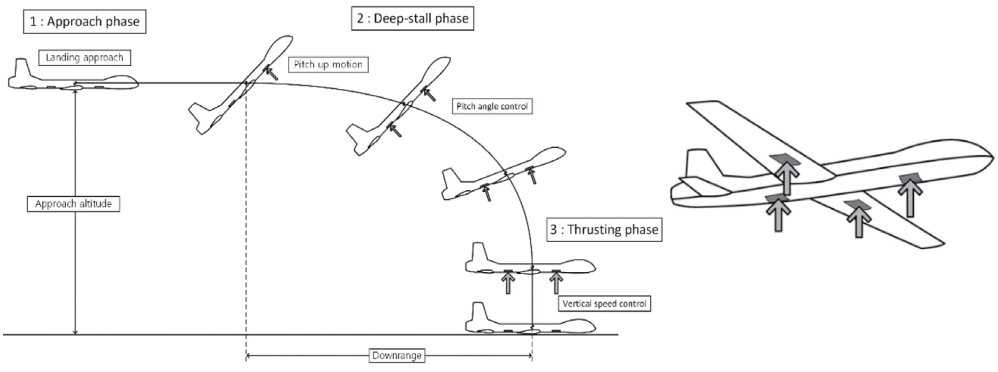

Fig. 1. (a) PLAT maneuver concept, (b) Thruster configuration

of four thrusters: two thrusters at the left/right wingspan for lateral control and the two at the front/back fuselage for longitudinal control. Any kind of thruster – e.g. solid propellant motor, cold gas thruster, and reaction thruster – that can create required magnitude of force is suitable for PLAT. In this paper, the solid propellant rocket is selected as a reference with the following two assumptions: 1) the level of thrust is continuous, and 2) the thruster can be switched on and off repeatedly.

Detail explanations on phases of the proposed landing maneuver are elucidated as follows. During approach phase, vehicle horizontally approaches the desired landing position. Firstly, the speed and height of the aircraft must be higher than the certain safe value in this phase. Then making the plane to fall in the deep stall, elevator input and thruster create large pitch up moment during deep stall phase. While the aircraft is in deep-stall, four thrusters and control surfaces will be controlled to retain proper pitch angle. It makes the largest possible drag during maintaining a stability. Lastly, to softly land on the desired position, four thrusters will propel the aircraft upward when the vehicle reaches the pre-calculated certain velocity and height in thrusting phase. From results of existing studies, the bang-off-bang control is known to be the best strategy that minimizes the overall control efforts [2,3,5]. Consequently, the maximum allowable thrust level will be used during thrusting phase.

Compared to other landing methods, the PLAT method has several advantages as follows. First, a precision landing on with a very limited space is possible. It does not need an open, long and large runway as other landing methods do. It is also applicable to various size fixed wing aircrafts depending on the specification of thruster used. Furthermore, using thrusters makes whole system relatively stable, in particular compared with conventional perching method with aerodynamic force only, which is exposed to high nonlinearity and uncertainty. Finally, PLAT can be adopted by currently operating platform with minor adjustments such as addition of thrusters and revision of flight software algorithm.

2.2 Aircraft Modeling

For PLAT simulation, some parameters of the unmanned aerial vehicle 'RQ-7B Shadow 200', which is conventional fixed wing type aircraft with high wing, constant chord and pusher configuration, are used. As details of parameters are unavailable, those are estimated via approximated three dimensional model as shown in Fig. 2.

According to importance, to estimate the mass property like center of mass and moment of inertia aircraft model is divided into four parts; main wing, tail wing, frontal body and rare body which includes engine. Based on existing data of similar UAV and existing works [16], mass portion of each subpart is set. m_{wing}=0.4$m_{A/C}$, m_{tail}=0.15$m_{A/C}$, $m_{f\text{-}body}$=0.25$m_{A/C}$ and $m_{r\text{-}body}$=0.2$m_{A/C}$ are used in this paper. To complete the realistic inertia model, additional mass from the installation of thrusters should be considered. Later at section 4.3, effects due to variation of mass will be considered. The form of each subpart is estimated as follows; main wing as NACA4415 airfoil with rectangular wing, tail wing as NACA0015 airfoil with V-tail and fuselage as round nose tapered cylinder. Software program 'Solidworks' is used to construct three dimensional model and to compute moment of inertia. Details of aircraft parameters after 3D model estimation are listed at Table 1.

In this research, two propellant thrusts and elevator are modeled as control actuator to satisfy the soft landing condition. The operation ranges and/or magnitude of each actuator are summarized at Table 2. The range of elevator are

Fig. 2. 'RQ-7B shadow 200' 3D model

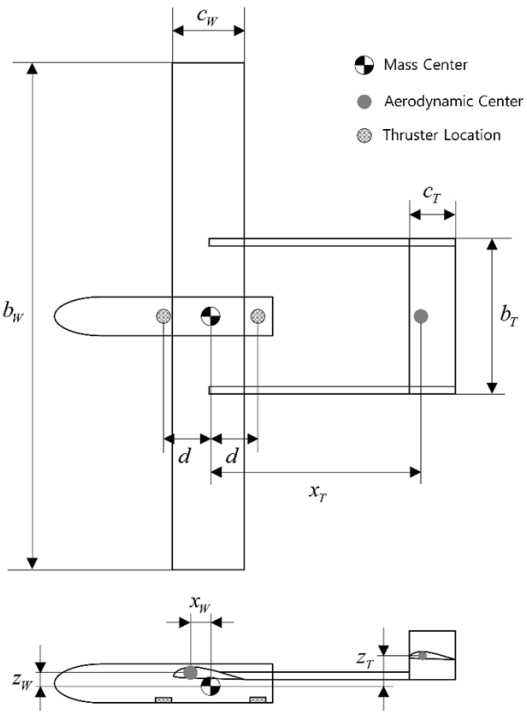

Fig. 3. 'RQ-7B shadow 200' top and side view

limited from -20 deg to +20 deg and its actuator dynamic is ignored. Detail aerodynamic characteristic variation due to elevator will be explain at aerodynamic modeling section. For the case of thruster, each one can sustain up to aircraft weight and general solid rocket specific impulse value is used.

2.3 Aerodynamic Modeling

From section 2.2, airfoil of the main wing and tail wing of 'RQ-7B Shadow 200' are respectively assumed to be NACA4415 and NACA0015. At Fig. 4-(a) and 4-(b), experimental aerodynamic coefficient data of each airfoil is marked. Aerodynamic data at high angle of attack are required to approximate the PLAT method accurately. Only information of NACA0015 at high angle of attack are known from research [17] and that of NACA4415 are limited from -17deg to 20deg.

Similarity in aerodynamic characteristics after deep stall between each different airfoil is shown by experiment results of [17]. Aerodynamic coefficient of NACA4415 at high angle of attack is approximated by sigmoid function $\sigma(\alpha)$ as a mixing function from experimental data. Similar to research [11], equation in (1) is used as sigmoid function where α_0 stands for the cut-off angle of attack and M represents the transition rate. Graph of $\sigma(\alpha)$ at α_0=20° and M=20 is shown in Fig. 4-(c).

$$\sigma(\alpha)=\frac{1+e^{-M(\alpha-\alpha_0)}+e^{M(\alpha+\alpha_0)}}{\left(1+e^{-M(\alpha-\alpha_0)}\right)\left(1+e^{M(\alpha+\alpha_0)}\right)} \tag{1}$$

Usually aerodynamic coefficients modeling is conducted by perturbation theory like equation (2), which approximates the coefficients using first order Taylor series expansion. Due to highly nonlinear effects after stall region, however, the methods are only able to work on low angle-of-attack. This paper estimates the aerodynamic coefficients at high angle-of-attack based on experimental data with interpolation rather than using perturbation theory directly.

$$C_X=C_{X_0}+C_{X_\alpha}\alpha+C_{X_T}\left(\frac{V}{V_0}\right)+C_{X_{\dot\alpha}}\left(\frac{\bar c}{2V_0}\right)\dot\alpha+C_{X_q}\left(\frac{\bar c}{2V_0}\right)q+C_{\delta_{elv}}\delta_{elv},\ X=L,D,m \tag{2}$$

In this paper, the longitudinal motion of the PLAT maneuver is dealt only to simplify the aerodynamic model, so any lateral motion or lateral forces is neglected. Also, any uncertainty or unsteady term in aerodynamic and fuselage

Table 1. 'RQ-7B shadow 200' 3D model data

Aircraft parameter		Value	Unit
m	Gross weight	140	kg
I_{yy}	Moment of inertia	90.135	$\mathrm{kg\cdot m^2}$
S_W	Wing platform area	1.649	$\mathrm{m^2}$
S_T	Tail wing area	0.31	$\mathrm{m^2}$
c_W	Wing chord length	0.485	m
c_T	Tail chord length	0.31	m
x_W	Main wing A.C to C.G length	0.13	m
z_W	Main wing A.C to C.G height	0.0	m
x_T	Tail wing A.C to C.G length	1.3	m
z_T	Tail wing A.C to C.G height	0.1	m
d	Thrust to C.G arm length	0.5	m
i_W	Wing incidence angle	0	deg
i_T	Tail incidence angle	-3	deg
τ	Elevator effectiveness ratio	0.35	1
η	Tail effectiveness ratio	0.85	1

Table 2. Actuator parameters

Actuator parameters		Value	Unit
δ_e	Elevator angle	-20 ~ +20	deg
T_P/W	Maximum thrust to weight ratio of each thruster	1	1
Isp	Specific impulse	240	sec

effects is ignored. Thereby, using the sigmoid function where X represents typical aerodynamic force and/or moment, aerodynamic model of main wing can be modeled as (3). Well known elevator derivative is integrated through tail angle of attack variation to take account of the effect of the elevator as equation (4).

$$C_{X_w}(\alpha_w)=\left(1-\sigma(\alpha_w)\right)C_{X_{NACA4415}}+\sigma(\alpha_w)C_{X_{NACA0015}},\ X=L,D,m \tag{3}$$

$$\begin{aligned} C_{X_T}(\alpha_T,\delta_{elv}) &\approx C_{X_{T0}}+C_{X_{T\alpha}}\alpha_T+\frac{dC_{X_T}}{d\delta_{elv}}\delta_{elv} \\ &= C_{X_{T0}}+C_{X_{T\alpha}}\alpha_T+\frac{dC_{X_T}}{d\alpha_T}\frac{d\alpha_T}{d\delta_{elv}}\delta_{elv} \\ &= C_{X_{T0}}+C_{X_{T\alpha}}\alpha_T+C_{X_{T\alpha}}\tau\delta_{elv} \qquad ,\ X=L,D,m \\ &\approx C_{X_T}(\alpha_T+\tau\delta_{elv}) \\ &= C_{X_{NACA0015}}(\alpha_T+\tau\delta_{elv}) \end{aligned} \tag{4}$$

Due to local change in the angle of attack, the dynamic stability derivatives about pitch rate are approximated according to the change of aerodynamic coefficients in many cases. Thereby, using local angle of attack can include effects of pitch rate rather than derivatives. Then, local angle of attack is derived from angle between body x-axis and local velocity vector as equation (5); where $\vec{V}_{rel}$, $\vec{q}$, $\vec{r}$, W and T represent the velocity of aircraft, pitch rate vector, vector from center of mass to aerodynamic center, main wing and tail wing respectively.

$$\vec{V}_x=\vec{V}_{rel}+\vec{q}\times\vec{r}_x,\ \ \alpha_x=\theta-\gamma_x,\ \ \ x=W,T \tag{5}$$

Finally, as the PLAT method needs the angle of attack up to 90 deg, which highly differs from usual case, small angle approximation is not used. Also, moment due to drag is not negligible for the same reason as above. From this, overall aerodynamic model can be constructed as equation (6)-(8). The total lift, drag and moment coefficients, plotted versus angle of attack at center of mass when elevator deflection angle are δ_{elv}=0, -20, +20deg, are shown in Fig. 5. Similarly, Fig. 6 present aerodynamic coefficient graph when V=25m/s and q=±0.5rad/s respectively.

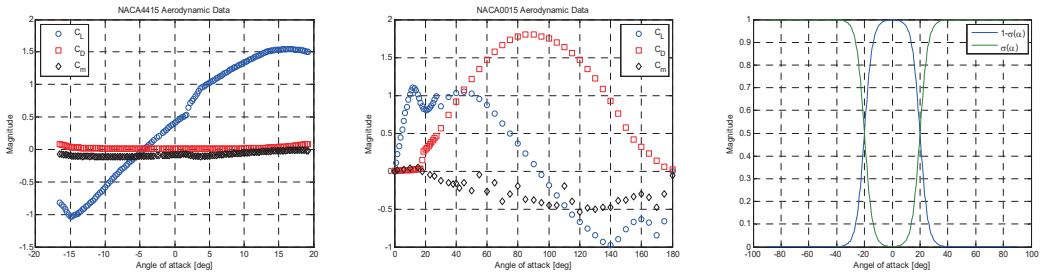

Fig. 4. (a) NACA4415 Aero-coeffcient, (b) NACA0015 Aero-coeffcient, (c) Sigmoid function

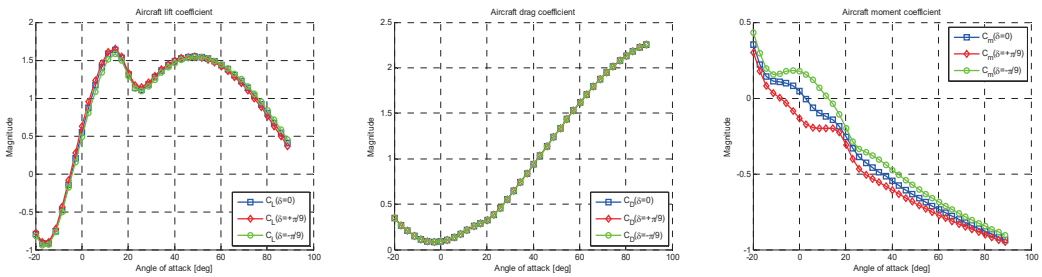

Fig. 5. Aircraft aerodynamic coefficient (a) Lift (b) Drag (c) Moment with elevator effects

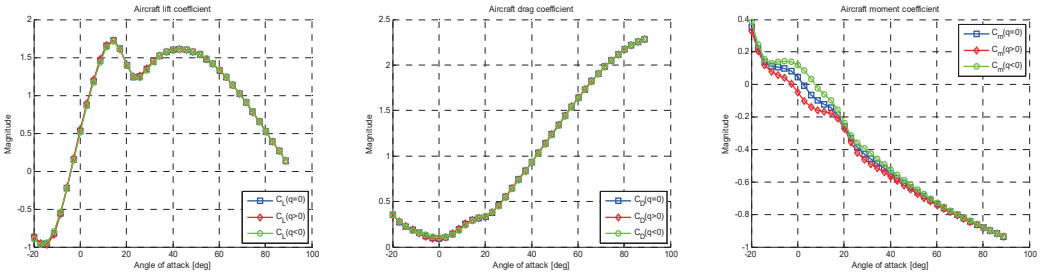

Fig. 6. Aircraft aerodynamic coefficient (a) Lift (b) Drag (c) Moment with pitch rate effects

DOI: http://dx.doi.org/10.5139/IJASS.2016.17.3.378

$$C_L(\alpha_W,\alpha_T,\delta_{elv}) = C_{L_{B0}} + \frac{1}{S_W}\left(S_W C_{L_W}(\alpha_W) + \eta S_T C_{L_T}(\alpha_T + \tau\delta_{elv})\right) \quad (6)$$

$$C_D(\alpha_W,\alpha_T,\delta_{elv}) = C_{D_{B0}} + \frac{1}{S_W}\left(S_W C_{D_W}(\alpha_W) + \eta S_T C_{D_T}(\alpha_T + \tau\delta_{elv}) + \frac{C_{L_W}^2}{\pi e_W AR_W} + \frac{\eta^2 C_{L_T}^2}{\pi e_T AR_T}\right) \quad (7)$$

$$C_m(\alpha_W,\alpha_T,\delta_{elv}) = C_{m_{B0}} + \frac{1}{c_W S_W}\left\{c_W S_W C_{m_W} + x_W\left(S_W C_{L_W}\cos\alpha_W + S_W C_{D_W}\sin\alpha_W\right) + \eta\left(c_T S_T C_{m_T} - x_T\left(S_T C_{L_T}\cos\alpha_T + S_T C_{D_T}\sin\alpha_T\right) + z_T\left(-S_T C_{L_T}\sin\alpha_T + S_T C_{D_T}\cos\alpha_T\right)\right)\right\} \quad (8)$$

From above Figure, the variation of lift, drag and moment coefficients due to elevator deflection or pitch rate are observed. The change of lift and drag is subtle as majority of total lift and drag comes from main wing and length from center of mass to aerodynamic center of main wing is negligible. In case of moments, however, it varies considerably as affected greatly by tail wing. As shown in Fig. 5-(c), the positive elevator deflection creates negative moment variation and vice versa. In case of pitch rate effects on moment, positive pitch rate generates negative pitch moment and vice versa. This results coincide with well-known elevator/tail damping effects, and similar to aerodynamic model from related research [7 8].

3. Trajectory Optimization

3.1 Optimal Control Problem Formulation

The amount of propellant requirement during landing is one of the most important things not sure to validate the realistic possibility of the suggested landing method, PLAT. In that sense, the objective function is formulated to minimize the overall thruster input in this paper. Then, cost function is set as follows. In here, T_{P1} and T_{P2} denote magnitude of frontal and rare thrust respectively.

$$J = \int_{t_0}^{t_f}\left(T_{P1} + T_{P2}\right)dt \quad (9)$$

To construct a dynamic model detail enough to reflect real motion while not too complicated to express, the aircraft is assumed as a rigid body and dynamic response of the thruster is neglected due to its fast response. Also, any lateral motion or lateral forces is neglected as mentioned before. Related longitudinal equations of motion can be set as equation (10)-(16) referring to Fig. 7 with these assumptions. V, γ, θ, q, x, and h stand for flight speed, flight path angle, pitch angle, pitch rate, downrange and altitude of the vehicle, respectively. Calculated from the equation (6)-(8), C_L, C_D and C_m represent the lift, drag and moment coefficients of the aircraft. Finally, Q and α each stands for the dynamic pressure and angle of attack, respectively.

$$\dot{V} = \frac{1}{m}\left(-QS_W C_D(\alpha_W,\alpha_T,\delta_{elv}) - W\sin\gamma - (T_{P1}+T_{P2})\sin\alpha\right) \quad (10)$$

$$\dot{\gamma} = \frac{1}{mV}\left(QS_w C_L(\alpha_w,\alpha_t,\delta_{elv}) - W\cos\gamma + (T_{P1}+T_{P2})\cos\alpha\right) \quad (11)$$

$$\dot{\theta} = q \quad (12)$$

$$\dot{q} = \frac{1}{I_{yy}}\left(QS_w c_w C_m(\alpha_w,\alpha_t,\delta_{elv}) + (T_{P1}-T_{P2})d\right) \quad (13)$$

$$\dot{x} = V\cos\gamma \quad (14)$$

$$\dot{h} = V\sin\gamma \quad (15)$$

$$\alpha = \theta - \gamma \quad (16)$$

At the approach phase, the initial condition for the PLAT maneuver is determined when the vehicle is assumed to do trimmed level flight. Trim condition of stall speed may be one of the good options of the initial conditions, however the other initial conditions may exist resulting less cost than that. From this point of view, the initial conditions are set as the solutions of nonlinear algebraic trimmed level

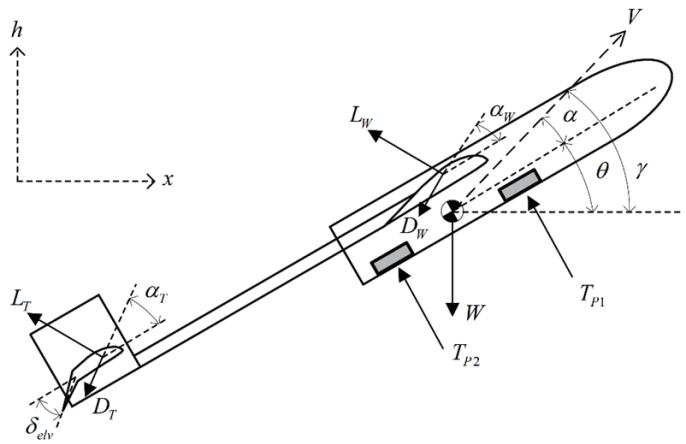

Fig. 7. Free body diagram of PLAT maneuver

flight equation. In case of initial height, various values are simulated and the tendencies of each simulation results are compared at later section.

$$\dot{\gamma} = \frac{1}{mV}\left(QS_w C_L\left(\alpha_0, \alpha_0, 0\right) - W\right) = 0 \tag{17}$$

$$\dot{\theta} = q = 0 \tag{18}$$

$$\dot{q} = \frac{1}{I_{yy}} QS_w c_w C_m\left(\alpha_0, \alpha_0, 0\right) = 0 \tag{19}$$

$$\theta_0 = \alpha_0 \tag{20}$$

To achieve criteria of the soft landing, the terminal speed of the vehicle must be near zero when altitude is zero. Furthermore, the pitch angle and pitch rate must be near zero when the aircraft does touch-down, while flight path angle should be about -90 degree to make trajectory steep. The terminal condition for downrange is not important as the other conditions, but it is needed to be specific not to glide. In this paper, terminal downrange is set as 90m and the terminal condition satisfying perch landing can be specified as follows. To ease the computation complexity, some terminal states such as velocity, flight path angle, pitch angle and pitch rate are bounded by inequality constraints. Such terminal boundaries are small enough to satisfy soft landing condition.

$$\begin{array}{lll} V\left(t_f\right) \le 0.1\,\text{m/s}, & \left|\gamma\left(t_f\right) + \pi/2\right| \le 0.05\,\text{rad} & \left|\theta\left(t_f\right)\right| \le 0.05\,\text{rad} \\ \left|q\left(t_f\right)\right| \le 0.05\,\text{rad/s}, & x\left(t_f\right) = 90\,\text{m} & h\left(t_f\right) = 0\,\text{m} \end{array} \tag{21}$$

3.2 Optimization results

The pseudo-spectral method (PSM) is used to solve the formulated optimal control problem. The PSM parametrizes both of control and state vectors at selected collocation points and thereby converts a dynamic optimization problem to a nonlinear programming problem. The optimal control problem was implemented in MATLAB and GPOPS-II is used to solve the problem [14]. Lower/Upper bounds of the state and control variables are carefully chosen, based on the dynamic characteristics of the airplane. The bounds of states and control variables having physical meaning are listed in Table 3 and are used to compute. Flight path angle is constrained in order not to UAV to go backward and pitch angle is bounded for safe operating envelope. In case of control variables, maximum thrust value is set as UAV's weight and elevator deflection angle are restricted.

Results of the optimal control optimal control problem that minimizing the overall propellant consumption are plotted through Fig. 8–9. The initial and terminal state values of the optimal trajectory are listed in Table 4 and trajectory characteristics are at Table 5.

The results show that aircraft does trimmed level flight with condition satisfying nonlinear algebraic equation (17)-(20) which corresponds to the approach phase. After that, the aircraft falls into deep stall as pitch angle increases drastically by frontal thruster usage. At the same time, elevator is deflected to -20 degrees to generate positive pitching moment resulting minimization of thruster usage. Pitch angle is controlled to be near 90 degrees for maximizing the drag and consequently to reduce velocity effectively, which corresponds to deep stall phase. Also during this phase, only frontal thruster is used as on/off controller with consideration of states hysteresis to make the angle of attack to oscillate around 90 degrees. Lastly, both frontal and rear thrusters are fully operated until just before the touch down after initiation, which corresponds to the thrusting phase. In this phase, there exists time offset between the initiation of frontal thruster and that of rear thruster to meet terminal pitch rate bounds while eliminate remaining velocity. In addition, elevator deflection angle is reversed to +20 degrees to generate negative pitching moment. Comparing the results with related previous research [3,4] and well known moon lander problem [12,13] validates that control alike bang-off-bang is optimal.

Physical meaning of computed optimal cost is the total impulse generated from thruster. From following equation (22), the amount of propellant requirement can be estimate. With given thruster data and calculated optimal cost, as listed in Table 5, the required propellant mass is about which is only 1.42% of total aircraft weight.

Table 3. Lower/Upper Bounds of Variables

State variable	Lower bound	Upper bound	Unit
γ	$-\pi/2$	$\pi/2$	rad
θ	$-\pi/4$	$\pi/2$	rad
Control variable	Lower bound	Upper bound	Unit
T_{P1}	0	$W \approx 1370$	N
T_{P2}	0	$W \approx 1370$	N
δ_{elv}	–20	20	deg

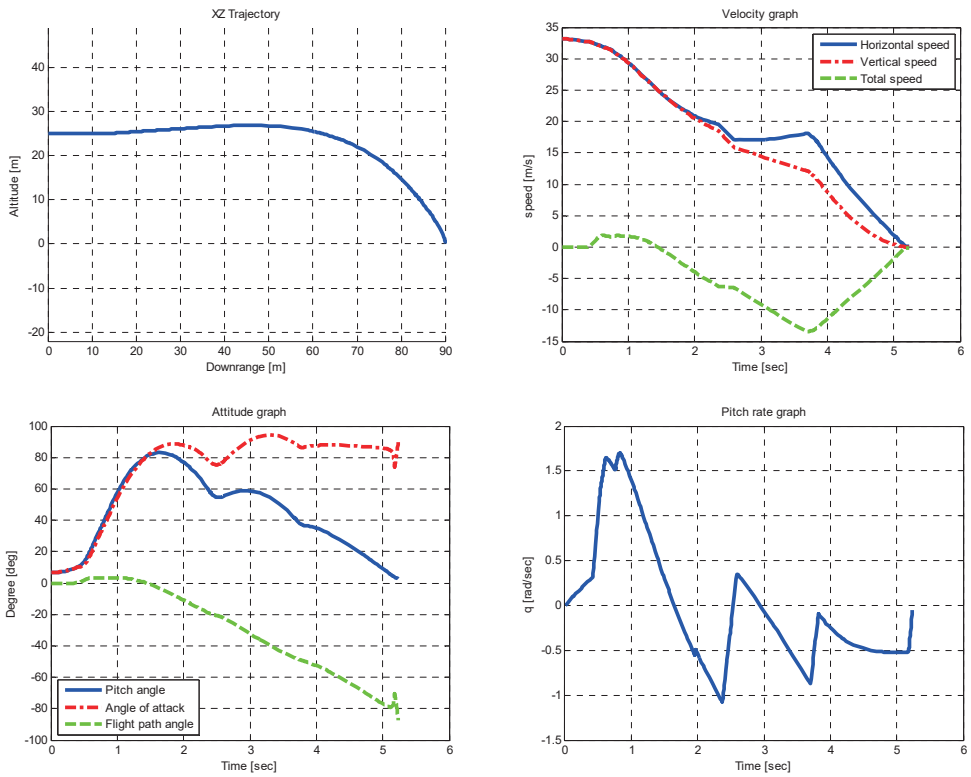

Fig. 8. Optimal (a) Trajectory, (b) Velocity, (c) Angle, (d) Pitch rate history

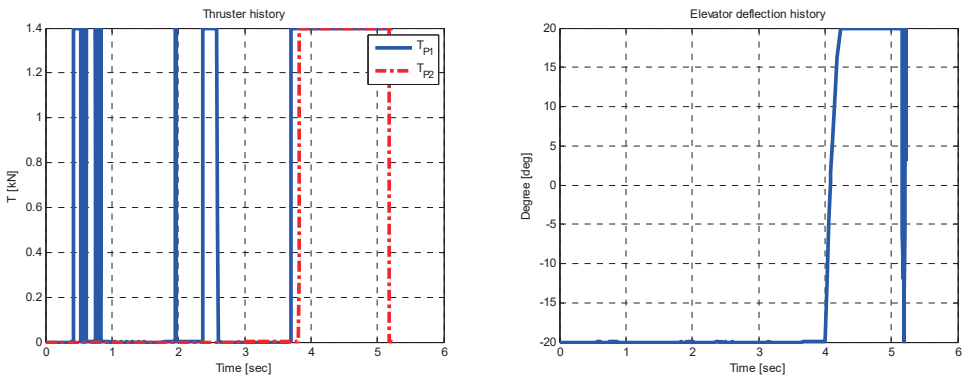

Fig. 9. Optimal (a) Thrust, (b) Elevator history

Table 4. Initial/Terminal Conditions of Trajectory

State variable	Initial condition	Terminal condition		Unit
V	33.2083	0.1	$(V(t_f) \le 0.1)$	m/s
γ	0	−1.5208	$(\lvert\gamma(t_f) + \pi/2\rvert \le 0.05)$	rad
θ	0.1150	0.05	$(\lvert\theta(t_f)\rvert \le 0.05)$	rad
q	0	−0.05	$(\lvert q(t_f)\rvert \le 0.05)$	rad/s
x	0	90	$(x(t_f) = 90)$	m
h	25	0	$(h(t_f) = 0)$	m

$$J^* = \int_0^{t_f} \left(T_{P1} + T_{P2}\right) dt = I^* = Isp \cdot m^*_{fuel} \cdot g \tag{22}$$

4. Parametric Study

A parametric study exploring the impacts of the variations in important modeling parameters was conducted. The results for variations in initial altitude, maximum thrust level and weight of UAV are presented in the following subsections.

4.1 Variation of Initial Height

The change of the trajectory, when variation of initial height exists while fixing the maximum thrust level to 1W and assuming 'Zero-mass' thruster, indicates that variation of the initial height alters an entrance time to the deep stall phase and a duration of the phase. Fig. 10 shows overall optimal states and control history of each different initial height. The cost of trajectories for each different initial height are calculated at Table. 6. Based on those results, it turns out that cost variation is much smaller than the variation of the initial height. The change of initial height alters both an entrance time to the deep stall phase and a duration of the phase. Higher initial height results faster terminal velocity of deep stall phase (which is same as initial velocity of the thrusting phase), due to slightly longer free fall duration, making more usage of the thrust. However, the increase of deep stall phase duration compensates an additional cost requirement from longer free fall well enough, resulting lower cost increase.

4.2 Variation of Maximum Thrust Level

The change of the trajectory, when variation of Thrust to Weight Ratio(TWR) exists while fixing initial height to 25m and assuming 'Zero-mass' thrusters, indicates that variation of the TWR is not affecting the overall trajectory too much as variation of initial height does. Fig. 12. shows overall optimal states and control history of each different TWR. The cost of trajectories for each cases are calculated at Table. 7. Based

Table 5. Characteristics of Trajectory

Terminal time [sec]	Optimal Cost [N·sec]	Propellant requirement [kg]
5.2389	4648.1	1.9742

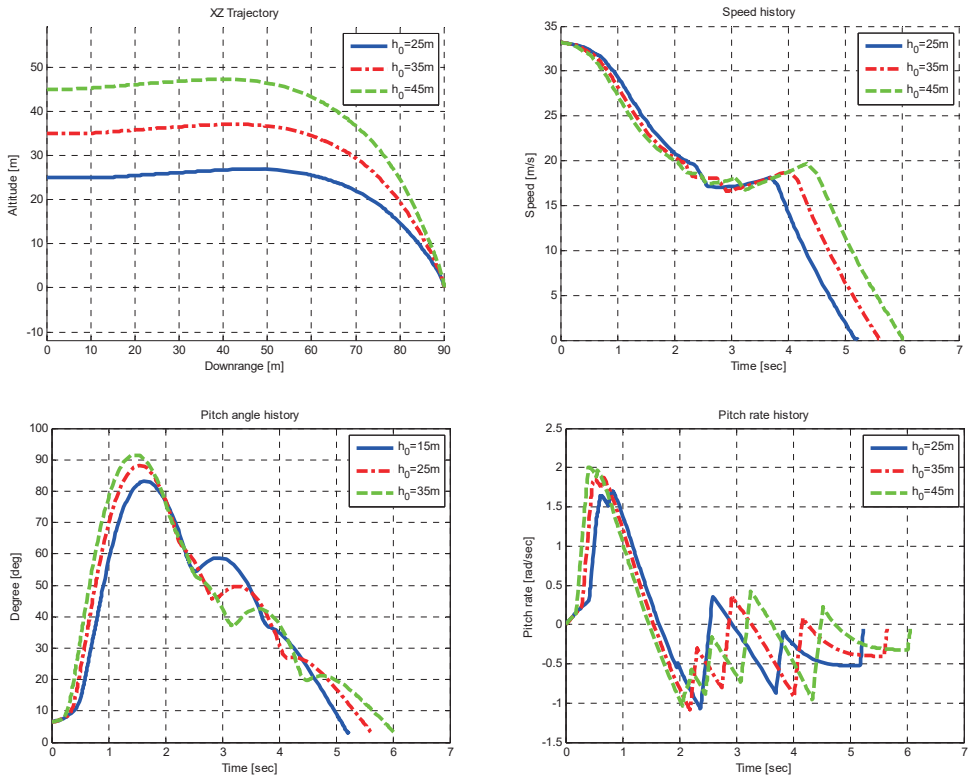

Fig. 10. Optimal (a) Trajectory, (b) Velocity, (c) Angle, (d) Pitch rate history for different initial height

on those results, it turns out that TWR variation does not alter optimal trajectory but makes thrust duration decrease resulting less fuel consumption. From previous analysis, ideal impulse like thrust (unbounded thrust input) is the best TWR that minimizes the overall cost.

4.3 Variation of UAV weight

As thrusters are added, additional supplement including the thrust itself will increase both mass and moment of inertia. To handle those uncertain inertia value, optimization under mass variation is conducted. In this paper, point mass

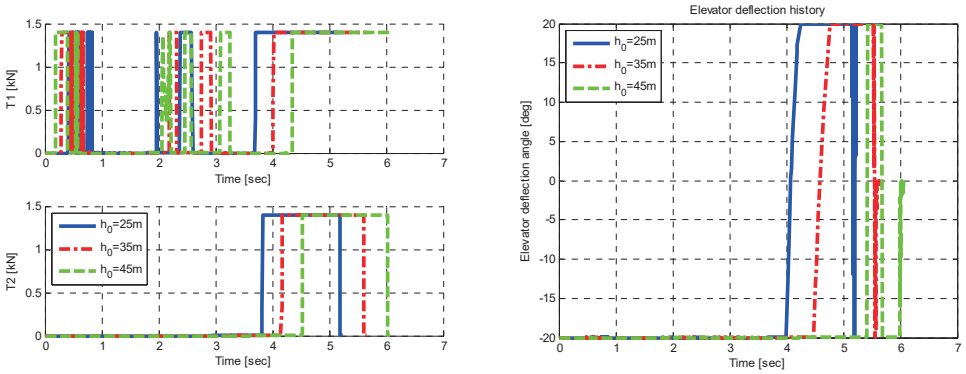

Fig. 11. Optimal (a) Thrust, (b) Elevator history for different initial height

Table 6. Characteristics of Trajectory for different initial height

Initial height [m]	25	35	45
Terminal time [sec]	5.2389	5.6484	6.0558
Optimal Cost [N·sec]	4648.1	5013.0	5339.3
Propellant requirement [kg]	1.9742	2.1292	2.2678

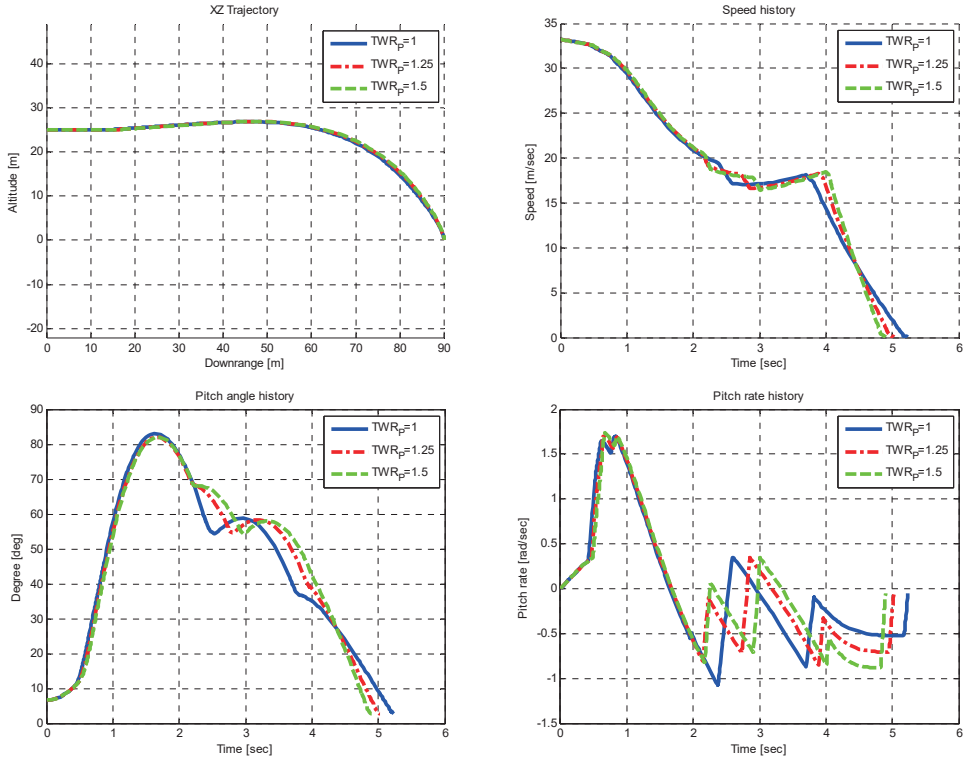

Fig. 12. Optimal (a) Trajectory, (b) Velocity, (c) Angle, (d) Pitch rate history for different thrust level

assumption is used for thrusters to make computation of mass and moment of inertia variation simple. The results, when considering mass of thrusters while fixing initial height to 25m and maximum thrust level to 1W, are computed for comparison.

Figure 14. shows overall optimal states and control history of each different inertia value. The cost of trajectories for each case are calculated at Table. 8. Based on those results, it turns out that inclusion of the additional mass from thrusters do not alter overall trajectory shape but degrades the overall

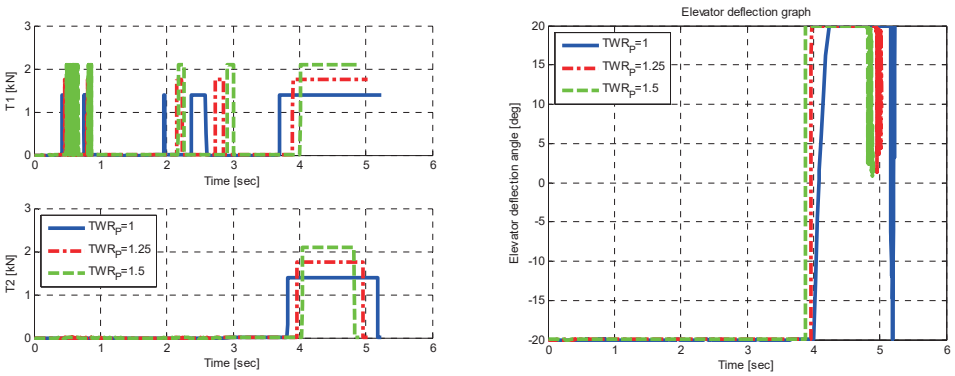

Fig. 13. Optimal (a) Thrust, (b) Elevator history for different thrust level

Table 7. Characteristics of Trajectory for different thrust level

Thrust level $[\mathrm{N}]$	$W \approx 1370$	$1.25W \approx 1710$	$1.5W \approx 2060$
Terminal time $[\mathrm{sec}]$	5.2389	5.0199	4.8962
Optimal Cost $[\mathrm{N}\cdot\mathrm{sec}]$	4648.1	4336.1	4166.4
Propellant requirement $[\mathrm{kg}]$	1.9742	1.8417	1.7696

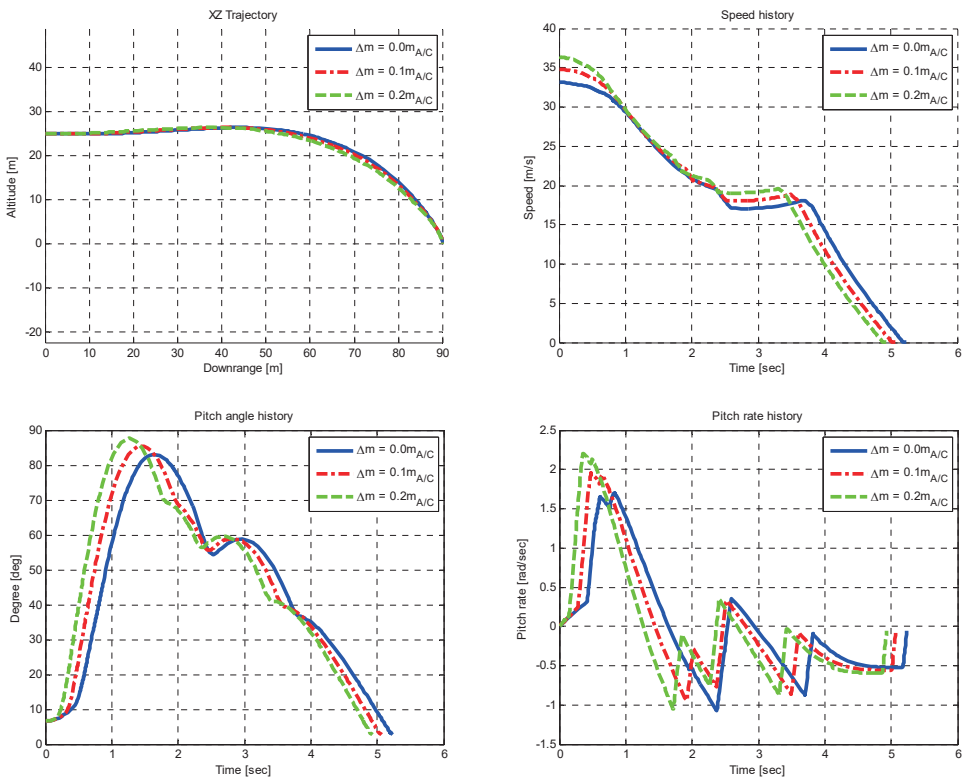

Fig. 14. Optimal (a) Trajectory, (b) Velocity, (c) Angle, (d) Pitch rate history for additional mass

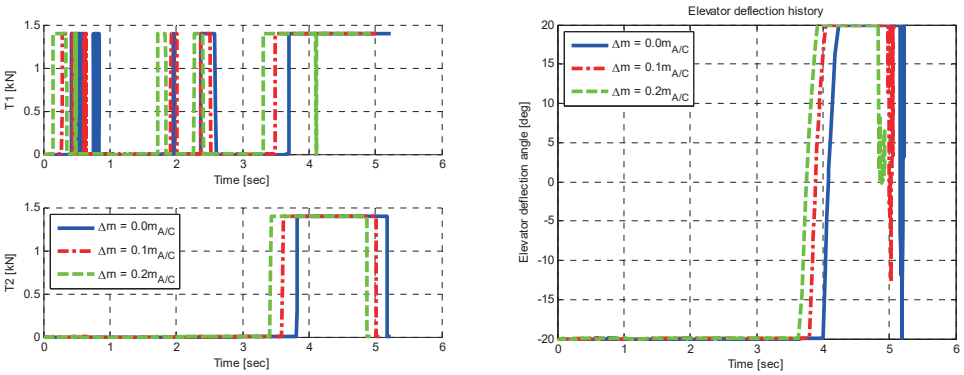

Fig. 15. Optimal (a) Thrust, (b) Elevator history for additional mass

Table 8. Characteristics of Trajectory for additional mass

Additional Mass	$\Delta m = 0.0 m_{A/C}$	$\Delta m = 0.1 m_{A/C}$	$\Delta m = 0.2 m_{A/C}$
Terminal time $[\text{sec}]$	5.2389	5.0680	5.2389
Optimal Cost $[\text{N}\cdot\text{sec}]$	4648.1	5279.1	5937.4
Propellant requirement $[\text{kg}]$	1.9742	2.2422	2.5218

performance of PLAT maneuver. Even if 20% of additional mass is considered, which is sufficient enough to cover the uncertain mass, optimization results show that such landing maneuver is possible.

5. Conclusion

In this paper, the concept of perch landing assisted by thrusters (PLAT) is proposed and analyzed. To validate a realistic possibility, this research has developed a concrete model to describe complicate aerodynamic and dynamics. From the model, optimal control problem minimizing the overall thruster input is formulated and Gauss pseudo spectral method is used as an optimization method owing to the complexity of dynamic model. From the optimization results, feasibility and realistic possibility of PLAT is demonstrated. In addition, effects of key parameter variation, such as initial height, thrust per weight ratio and mass, are analyzed.

This paper has limitations; exclusion of lateral motion effects and any unsteady aerodynamic effects due to flow transition or thruster jet, and assumption of continuous and repeatable thrusters. In the future work, real time guidance law for longitudinal PLAT and consequent controller design will be dealt. As designing the controller, the way to treat uncertain aerodynamic effects and mass variation will be studied. After guidance law and controller design, six degrees of freedom case will be considered.

Although there exist limitations and long way to be studied, this paper is meaningful to suggest new way of landing for fixed wing. Furthermore, not only for the UAV landing but also the method is able to use on other fields such as air existent planet exploration and precise airdrop cargo transportation.

References

[1] Tahk, M. J., Lee, B. Y. and Han, S. Y., "Method and System of Vertical Take-Off and Landing for Unmanned Aerial Vehicle", Korean Patent 10-2015-0015295, 2014.

[2] Tahk, M. J., Han, S. Y., Lee, B. Y. and Ahn, J. M., "Trajectory Optimization and Control Algorithm of Longitudinal Perch Landing Assisted by Thruster", submitted to *European Control Conferences*, Denmark, 2016.

[3] Han, S. Y., Yogaswara, Y. H., Lee, B. Y., Tahk, M. J. and Ahn, J. M., "Trajectory Optimization of Longitudinal Perch Landing Assisted by Thruster", *Proceedings of the 12th YUST International Symposium*, Yanbian, China, 2015.

[4] Han, S. Y., Lee, B. Y., Yogaswara, Y. H., Tahk, M. J. and Ahn, J. M., "Algorithm of Longitudinal Perch Landing Assisted by Thruster for Fixed Wing UAV", *Proceedings of the KSAS Fall Conferences*, Jeju, Korea, 2016.

[5] Han, S. Y., Tahk, M. J. and Ahn, J. M., "Perch Landing Assisted by Thruster", *Proceedings of the KSAS Spring*

Conferences, Jeongseon, Korea, 2015.

[6] Crowther, W. "Perched Landing and Takeoff for Fixed Wing UAVs", *NATO AVT Symposium on Unmanned Vehicles for Aerial*, Ground and Naval Military Operations, 2000.

[7] Wickenheiser, A. and Garcia, E., "Optimization of Perching Maneuvers Through Vehicle Morphing", *Journal of Guidance, Control, and Dynamics*, Vol. 31, No. 4, 2008, pp. 815–823.

[8] Venkateswara Rao, D. M. K. K. and Go, T. H., "Optimization, Stability Analysis, and Trajectory Tracking of Perching Maneuvers", *Journal of Guidance, Control, and Dynamics*, Vol. 37, No. 3, 2014, pp. 879-888.

[9] Cory, R. and Tedrake, R., "Experiments in Fixed-Wing UAV Perching", *Proceedings of the AIAA Guidance, Navigation, and Control Conference*, AIAA (AIAA Paper 2008-7256), Reston, VA, 2008.

[10] Taniguchi, H., "Analysis of Deepstall Landing for UAV", *Proceedings of ICAS2008, ICAS*, 2008.

[11] W. Pointer, G. Kotsis, P. Langthaler, M. Naderhirn, "Using formal methods to verify safe deep stall landing of a MAV", *Digital Avionics Systems Conference (DASC), 2011 IEEE/AIAA 30th*, Seattle, WA, Oct., 2011.

[12] Bryson, A. E. and Ho, Y. C., *Applied Optimal Control*, Hemisphere Publishing, 1975, ch. 3.

[13] Kirk, D. E., *Optimal Control Theory; An Introduction*, Dover, New York, 1970, pp. 247-248.

[14] Rao, A. V., Benson, D. A., Darby, C., Patterson, M. A., Francolin, C., Sanders, I., et al. . Algorithm 902: GPOPS, a MATLAB software for solving multiplephase optimal control problems using the Gauss pseudospectral method, *ACM Transactions on Mathematical Software*, Vol. 37, No. 2, Article 22, 2010.

[15] Fahlstrom, P. and Gleason, T., *Introduction to UAV Systems*, 4th edition, Wiley, 2012, pp. 247-276.

[16] Cau, D., "Simulation of Search Over Terrain with Unmanned Aerial Vehicles", *AIAA Infotech@Aerospace Conference*, St. Louis, MO, 2011.

[17] Sheldahl, R. E. and Klimas, P. C., "Aerodynamic Characteristics of Seven Symmetrical Airfoil Sections through 180-Degree Angle of Attack for Use in Aerodynamic Analysis of Vertical Axis Wind Turbines", Sandia National Laboratories Rept. SAND80-2114, 1981.